Arab J Sci Eng (2014) 39:4119–4129
DOI 10.1007/s13369-014-0984-z

RESEARCH ARTICLE - MECHANICAL ENGINEERING

The Effects of Design Parameters on Performance and NO Emissions of Steam-Injected Diesel Engine with Exhaust Gas Recirculation

Görkem Kökkülünk · Güven Gonca · Adnan Parlak

Received: 4 October 2012 / Accepted: 15 March 2013 / Published online: 4 March 2014

Abstract In this study, an engine test with steam injection and EGR is conducted for investigating the effects of engine design parameters such as compression ratio (CR), charge temperature and pressure and equivalent ratio on a direct injection diesel engine performance and NO emissions using zero-dimensional single-zone combustion model. After the results obtained from the model are validated and well suited with those experimental studies of the diesel engines running with 20 % steam ratio and 10 % EGR, some important design parameters are investigated by using the theoretical model. As results, it was shown that effective efficiency, effective power and NO emissions increase with the increase of CR, inlet pressure for a constant equivalence ratio and inlet temperature. However, effective power and efficiency increase to certain values and then reduce, while NO emissions constantly decrease as the inlet pressure increases for various equivalence ratios.

Keywords Compression ratio · Design parameters · Steam injection · EGR · NO emission · Single-zone combustion model

الخلاصة

تم في هذه الدراسة إجراء اختبار المحرك مع الحقن بالبخار وإعادة تدوير الغاز العادم للتحقيق في آثار معاملات تصميم المحرك مثل نسبة الضغط، ودرجة حرارة وضغط الشحن ونسبة التكافؤ على أداء محرك ديزل ذا حقن مباشر وانبعاثات أكسيد النيتروجين باستخدام نموذج الاحتراق ذي منطقة واحدة وصفري البعد. وبعد التحقق من صحة النتائج المتحصل عليها من النموذج ومناسبتها تماما مع تلك الدراسات التجريبية من محركات الديزل التي تعمل مع 20٪ نسبة البخار و 10٪ إعادة تدوير غاز عادم، تم التحقيق في بعض معاملات التصميم الهامة باستخدام النموذج النظري. كما النتائج، فقد تبين أن الكفاءة الفعالة، والقوة الفعالة وانبعاثات أكسيد النيتروجين تزداد مع زيادة نسبة الضغط، وضغط المدخل لثابت نسبة التكافؤ ومدخل درجة الحرارة، ومع ذلك، فإن القوة الفعلية والكفاءة تزداد حتى قيم معينة ومن ثم تنخفض، في حين أن انبعاثات أكسيد النيتروجين تنخفض باستمرار عند زيادة ضغط المدخل لنسب التكافؤ المختلفة.

Abbreviations

EGR	Exhaust gas recirculation
CFD	Computational fluid dynamic
SFC	Specific fuel consumption
DI	Direct injection
S20+E10	20 % Steam injection and 10 % EGR
CR	Compression ratio
IT	Inlet temperature
IP-SER	Inlet pressure at same equivalence ratio
IP-SFA	Inlet pressure at same fuel amount
RGF	Residual gas fraction
m_1	Leak mass, g
m_{fb}	Mass of burned fuel, g
h_1	Enthalpy of combustion products, kJ/kg
C	Dimensionless constant
C_p	Specific heat of constant pressure of air fuel mixture, kJ/kgK
m_f	Total mass of the injected fuel, g

G. Kökkülünk (✉) · A. Parlak
Marine Engineering Department, Yildiz Technical University, Besiktas, Istanbul, Turkey
e-mail: gorkemkulunk@gmail.com

G. Gonca
Naval Architecture and Marine Engineering Department, Yildiz Technical University, Besiktas, Istanbul, Turkey

x_b	The rate of the total burned fuel mass to total mass of injected fuel
F_{st}	Stoichiometric fuel–air ratio by mass
Δh	Combustion enthalpy, kJ/kg
M_f	Molecular weight of fuel, kg/kmol
P_i	Injection pressure of fuel, bar
v_f	Specific volume of fuel, cm^3/g
A_{cyl}	Heat transfer area of cylinder, cm^2
T	The temperatures of the in-cylinder gas zone, K
T_w	The temperatures of the cylinder walls, K
h_{tr}	Heat transfer coefficient
p	In-cylinder pressure, bar
S_p	Mean piston velocity, m/s
v	Specific volume, cm^3/g
V	Volume, cm^3
B	Cylinder Bore, cm
S	Cylinder Stroke, cm
j	Ratio of half stroke to rod length
m_a	Mass of air, g
m_{fi}	Mass of injected fuel, g
ε	Molar fuel–air ratio
φ	The equivalence ratio
γ(n)	Gamma function
θ	Instant crank angle, degree
θ_{di}	Injection duration, degree
θ_{si}	Start of fuel injection, degree
θ_{db}	Burning duration, degree
θ_{sb}	Start of burning, degree
ω	Angular velocity, 1/rad

1 Introduction

The engine designers have to develop new technologies and determine optimal design parameters such as compression ratio (CR), inlet temperature (IT), inlet pressure at same equivalence ratio (IP-SER) and same fuel amount at the beginning of compression process in the cylinder as exhaust emissions released from diesel engines must be kept under the mandatory emissions regulation while maintaining power output and high efficiency.

Besides the new technologies, many optimization researches by engine designers were conducted by using various parameters such as IT and CR. Rakopoulos et al. [1] performed a parametric study of a comprehensive, two-zone, transient, thermodynamic model of a diesel engine so as to evaluate the effect of various parameters such as load and turbocharger characteristics. Jayashankara et al. [2] carried out a parametric study to investigate the effect of fuel injection timing and intake pressure on the performance of a diesel engine using computational fluid dynamic (CFD). Kim et al. [3] conducted parametric studies on combustion, emission, and performance characteristics due to the injection angle and advance injection timing. Controlling NO emissions in diesel engines is very important research areas in engine developing phases.

Various solutions have been proposed to reduce NO emissions such as water injection directly to combustion chamber, emulsified and fumigation to intake manifold or steam injection to intake manifold [4–15]. Another method to highly reduce NO emissions is exhaust gas recirculation (EGR) [16–26] despite its effect on worsening specific fuel consumption (SFC) [21,25,26]. Water injection method is commonly used to improve performance and NO emissions of diesel engines. This method could lead to deterioration lubrication oil and corrosion in the cylinder. In order to prevent these bad effects, electronically controlled steam injection system has been developed, recently [13].

Apart from the above literature survey, there is no study to investigate effects of engine design parameters on the performance and NO emissions of steam-injected diesel engine with EGR. Hence, in this study, a direct injection (DI) diesel engine equipped with an electronically controlled steam injection system developed by Parlak et al. [13,14] and coupled with EGR is used to compare the effects of engine design parameters such as CR, inlet pressure (at same equivalence ratio or same fuel amount) and IT on NO emissions, effective power and efficiency, and in-cylinder temperature and pressure.

Kökkülünk [27] found the optimum steam and EGR rates of 20 % steam mass fraction of fuel injected and 10 % EGR (S20+E10) at full-load conditions when considering reduction in NO emissions and performance parameters. In the present study, a zero-dimensional single-zone combustion model developed for S20+E10 DI diesel engine is used to investigate the effects of engine design parameters for various CRs, ITs and inlet pressures with same equivalence ratio and same fuel amount.

2 Experimental Setup

The experiments were carried out with a single cylinder, naturally aspirated and four-stroke diesel engine with a bowl in combustion chamber. The experimental setup is shown in Fig. 1.

In order to measure brake torque, the engine is coupled with a hydraulic-type dynamometer of 50 kW absorbing capacity using an “S”-type load cell with the precision of 0.1 N. Before starting the experiments, load cell is calibrated sensitively. Table 1 illustrates the errors in parameters and total uncertainties with 95 % confidence interval.

In this study, MRU Spectra 1600 L type and Bilsa Mod gas analyzers were used so as to measure exhaust gases. Before experiments, emission devices were calibrated. Table 2 illustrates the technical data of MRU 1600 L emission device.

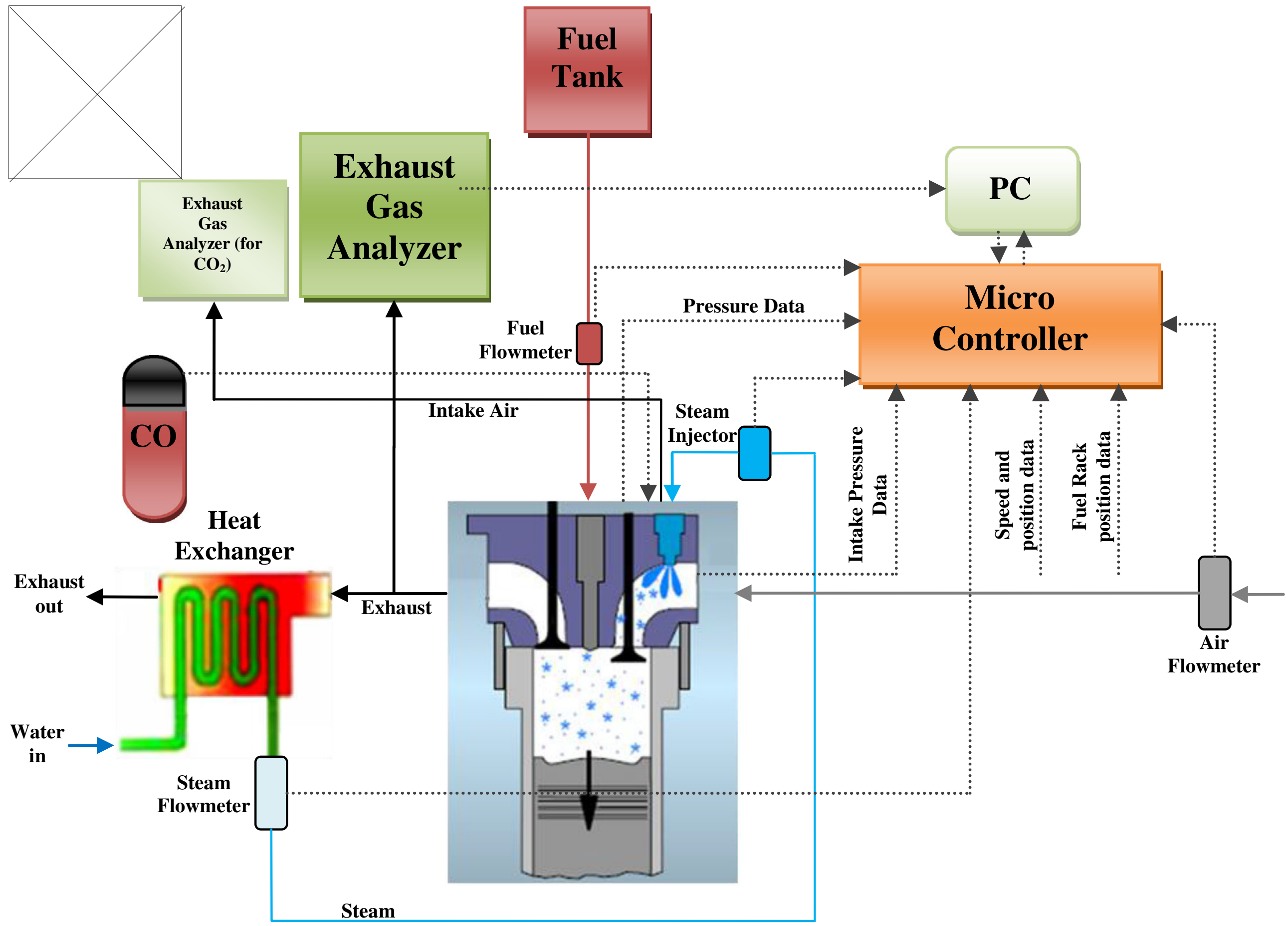

Fig. 1 Experimental setup

Table 1 The errors in parameters and total uncertainties with 95 % confidence interval

Parameters	Systematic errors
Load (N)	0.1
Speed (rpm)	1.0
Time (s)	0.1
Temperature (°C)	1
Fuel consumption (g)	0.5
	Total uncertainty (%)
Effective efficiency (%)	1.5
Effective power (kW)	1.1

Meanwhile, Table 3 shows the analysis of mean absolute percentage error (MAPE), root mean square error (RMSE) and standard deviation values of theoretical and experimental data.

So as to measure in-cylinder pressure, Kistler brand 6061B model, water cooled piezo-electric sensor and Kistler 5018 type charge amplifier were used in the single-cylinder engine. Smetec brand four-channel data card which has 1 MB data acquisition rate from a single-channel "Combi Combustion Indication System" was used for data transfer, and Koyo TRD J1000-RZ type encoder which has 1000 pulse/revolution was used in order to measure angular position.

99 % purity Linde Gas brand CO_2 gas was used for EGR application due to the most compound in exhaust gases and to calibrate EGR ratio.

Method of Needham et al. [28] was used in order to determine the amount of CO_2 gas. EGR percentage is

$$\text{EGE}\ (\%) = \frac{CO_{2(\text{intake\_manifold})} - CO_{2(\text{surroundings})}}{CO_{2(\text{exhaust\_manifold})}} \times 100 \quad (1)$$

where $CO_{2(\text{surroundings})}$ is the reference CO_2 percentage in surroundings. In this study, this value was neglected owing to being 0.03 % in the literature [29]. EGR ratios were determined with a volume ratio of CO_2 value. In the experiments, 10, 20 and 30 % EGR ratios were carried out.

Table 2 Technical data of MRU 1600 L emission device

Measured parameters	Unit	Measuring range	Measured precision
CO	%	0–15.0 %	±0.06 % or ±5 % of measured value
CO_2	%	0–20.0 %	±0.5 % or ±5 % of measured value
HC (*n*-hexane)	ppm	0–20,000	±12 ppm or ±5 % of measured value
NO	ppm	0–2,000	±5 ppm or ±5 % of measured value

Table 3 Analysis of MAPE, RMSE and standard deviation of theoretical and experimental data

	RMSE	MAPE	Standard deviation
Effective power	0.000002	0.0001	0.0017
Effective efficiency	0.000023	0.0001	0.0052
NO	0.083800	0.0006	0.2977

Experiments were done in variable speeds 1,200, 1,400, 1,600, 1,800, 2,000, 2,200 and 2,400 rpm at full-load conditions.

Saturated water which is in the condition of 3 bar pressure and 133.5 °C was injected into intake manifold via injector at intake period. During the injection period, water changed its phase from saturated condition to super heat condition by throttling with a constant enthalpy from 3 bar to about 1 bar. This phase eliminates the risk of corrosive side effects of water on a metallic surface by preventing condensation of water. Steam amount was determined by mass ratio of injected fuel.

3 Modeling Methodology

In the theoretical model [30], it is assumed that gas mixture is homogeneous in the engine cylinder; blow by coefficient, gas leakage and residual gas fraction is constant; and air–fuel mixture is an ideal gas.

In the cylinder, the energy equations in differential form may be written as [31].

$$\frac{dU}{d\theta} = \frac{dQ}{d\theta} + \frac{dW}{d\theta} + \frac{dm_{fb}}{d\theta}h_f - \frac{dm_1}{d\theta}h_1 \tag{2}$$

where m_1 is leak mass and m_{fb} is mass of burned fuel; h_f and h_1 are enthalpy of combustion products resulting from burned fuel and leak mass, respectively. The time (crank angle)-dependent burned gas leaking through the rings is

$$\frac{dm_1}{d\theta} = \frac{Cm}{\omega} \tag{3}$$

In this study, C is dimensionless constant and defines all the losses in the cylinder except the lost energy to the cooling fluid.

The mass rate of burned fuel can be stated as

$$\frac{dm_{fb}}{d\theta} = \frac{\dot{m}_{fb}}{\omega} \tag{4}$$

where $\dot{m}_{fb}$ is the crank angle-dependent burned fuel rate and it can also be given as

$$\dot{m}_{fb} = \dot{X}_b m_f \tag{5}$$

$$\frac{m_{fb}}{d\theta} = \frac{x_b}{d\theta} m_f \tag{6}$$

where m_f and x_b are the total mass of the injected fuel and the rate of the total burned fuel mass to total mass of injected fuel, respectively. The total mass of the injected fuel can be written as

$$m_f = \phi F_{st}(1 - \mathrm{RGF}) m_a \tag{7}$$

where RGF, ϕ and F_{st} are residual gas fraction, the equivalence ratio and the stoichiometric fuel–air ratio by mass, respectively. The rate of the total burned fuel mass to total mass of injected fuel could be given as

$$x_b = 1 - e^{-a_v\left(\frac{\theta-\theta_{sb}}{\theta_{db}}\right)^{(m_v+1)}} \tag{8}$$

$$\frac{dx_b}{d\theta} = a_v\left(\frac{\theta-\theta_{sb}}{\theta_{db}}\right)^{m_v}\left(\frac{m_v+1}{\theta_{db}}\right) e^{-a_v\left(\frac{\theta-\theta_{sb}}{\theta_{db}}\right)^{(m_v+1)}} \tag{9}$$

x_b is given as burning fraction. It is 0 at the start of combustion and it would be 1 at the end of combustion. It is determined according to experimental results. θ, θ_{sb} and θ_{db} are instant crank angle, crank angle at the start of burning and burning duration in crank angle, respectively.

The enthalpy of burned fuel could be expressed as

$$h_f = \Delta h / M_f + (P_i - 1.01325) v_f / 10 \tag{10}$$

where Δh, M_f, P_i and v_f are combustion enthalpy, molecular weight, injection pressure and specific volume of the fuel, their values are −174,000 kJ/kg, 199.15 kg/kmol, 150 bar and 1.189 cm^3/g, respectively.

The heat loss with respect to crank angle is given as

$$\frac{dQ}{d}\theta = -\frac{\dot{Q}_1}{\omega} \tag{11}$$

where ω is angular velocity and the heat loss rate can be obtained as following:

$$\dot{Q}_1 = h_{\mathrm{tr}} A_{\mathrm{cyl}} (T - T_{\mathrm{w}}) \tag{12}$$

where h_{tr}, A_{cyl}, T and T_{w} are heat transfer coefficient, heat transfer area of the cylinder, the temperatures of the in-cylinder gas zone and cylinder walls, respectively [31]. The heat transfer coefficient (h_{tr}) is found by using Hohenberg's [32] approach and written as below:

$$h_{\mathrm{tr}} = C_1 V^{-0.06} p^{0.8} T^{-0.4} (\bar{S}_{\mathrm{p}} + C_2)^{0.8} \tag{13}$$

where $C_1 = 130$, $C_2 = 1.4$, p, T and $\bar{S}_{\mathrm{p}}$ are in-cylinder pressure, temperature and the mean piston velocity in bar, Kelvin and meters per second, respectively. The crank angle-dependent statement of the work is given as

$$\frac{\mathrm{d}W}{\mathrm{d}\theta} = -p \frac{\mathrm{d}V}{\mathrm{d}\theta} \tag{14}$$

where p and V are in-cylinder pressure and volume. The change of cylinder volume depending on crank angle is the following:

$$\frac{\mathrm{d}V}{\mathrm{d}\theta} = \frac{\pi}{8} B^2 S \sin\theta \left[1 + j \frac{\cos\theta}{(1 - j^2 \sin^2\theta)^{\frac{1}{2}}} \right] \tag{15}$$

where B, S and j are the cylinder bore, stroke and the ratio of half stroke to rod length, respectively.

Mass balance within the cylinder can be expressed as follows;

$$m = m_{\mathrm{a}} + m_{\mathrm{fi}} \tag{16}$$

where m_{a} and m_{fi} are the masses of the air and injected fuel, respectively. If the Eq. (16) is written in differential form, it becomes as follows:

$$\frac{\mathrm{d}m}{\mathrm{d}\theta} = \frac{\mathrm{d}m_{\mathrm{a}}}{\mathrm{d}\theta} + \frac{\mathrm{d}m_{\mathrm{fi}}}{\mathrm{d}\theta} \tag{17}$$

The air and injected fuel rates changing with crank angle within the cylinder are expressed respectively as

$$\frac{\mathrm{d}m_{\mathrm{a}}}{\mathrm{d}\theta} = \frac{-\dot{m}_1/\omega}{1 + \phi F_{\mathrm{st}}} + \frac{-C m_{\mathrm{a}}}{\omega} \tag{18}$$

It is seen from Eq. (18) that the air mass decreases due to gas leak depending on C with respect to crank angle.

$$\frac{\mathrm{d}m_{\mathrm{fi}}}{\mathrm{d}\theta} = \frac{1}{\omega} \left(\dot{m}_{\mathrm{fi}} - \frac{\dot{m}_1 \phi F_{\mathrm{st}}}{1 + \phi F_{\mathrm{st}}} \right) = \frac{\dot{m}_{\mathrm{fi}} - C m_{\mathrm{fi}}}{\omega} \tag{19}$$

where $\dot{m}_{\mathrm{fi}}$ is the time-dependent injected fuel rate and it can also be expressed as

$$\dot{m}_{\mathrm{fi}} = \dot{x}_{\mathrm{i}} \mathrm{m}_{\mathrm{f}} \tag{20}$$

where $\dot{x}_{\mathrm{i}}$ is the fraction rate of the total mass of injected fuel, which can be given as

$$\dot{x}_{\mathrm{i}} = \frac{\omega}{\theta_{\mathrm{di}} \Gamma(n)} \left(\frac{\theta - \theta_{\mathrm{si}}}{\theta_{\mathrm{di}}} \right)^{n-1} \exp\left[\frac{-(\theta - \theta_{\mathrm{si}})}{\theta_{\mathrm{di}}} \right] \tag{21}$$

where θ_{di} is a parameter related to injection duration [31] and θ_{si} is crank angle at the start of fuel injection. Where $\Gamma(n)$ is the gamma function, it is written as [31]

$$\ln\Gamma(n) = \left(n - \frac{1}{2} \right) \ln(n) - n + \frac{1}{2} \ln(2\pi) + \frac{1}{12n} - \frac{1}{360n^3} + \frac{1}{1{,}260n^5} - \frac{1}{1{,}680n^7} \tag{22}$$

For the diesel engine with open chamber, the value of n could be taken as $1 \le n \le 2$ and for close chamber as $3 \le n \le 5$. But exact value is dependent on fuel used and engine design. The time (crank angle)-dependent expressions of pressure and mean gas temperatures are given respectively as [31]

$$\frac{\mathrm{d}p}{\mathrm{d}\theta} = \frac{-\frac{pv}{T}\left[\frac{10c_{\mathrm{p}}T}{pV} - \frac{\partial \mathrm{In}v}{\partial \mathrm{In}T} \right] \frac{\mathrm{d}v}{\mathrm{d}\theta} - \frac{10 \frac{\mathrm{d}u}{\mathrm{d}\theta} \frac{\partial \mathrm{In}v}{\partial \mathrm{In}T}}{P}}{\frac{v^2}{T}\left[\left(-\frac{10c_{\mathrm{p}}T}{pV} + \frac{\partial \mathrm{In}v}{\partial \mathrm{In}T} \right)\left(-\frac{\partial \mathrm{In}v}{\partial \mathrm{In}P} \right) + \left(\frac{\partial \mathrm{In}v}{\partial \mathrm{In}T} + \frac{\partial \mathrm{In}v}{\partial \mathrm{In}P} \right) \right]} \tag{23}$$

$$\frac{\mathrm{d}T}{\mathrm{d}\theta} = \frac{-v\left[\frac{10\left(\frac{\mathrm{d}u}{\mathrm{d}\theta}\right)}{P \frac{\partial \mathrm{In}v}{\partial \mathrm{In}P}} + \left(\frac{\mathrm{d}v}{\mathrm{d}\theta} \right)\left(\frac{\partial \mathrm{In}v}{\mathrm{In}T} + \frac{\partial \mathrm{In}v}{\mathrm{In}P} \right) \right]}{\frac{v^2}{T}\left[\left(-\frac{10c_{\mathrm{p}}T}{pv} + \frac{\partial \mathrm{In}v}{\partial \mathrm{In}T} \right)\left(-\frac{\partial \mathrm{In}v}{\partial \mathrm{In}p} \right) + \frac{\partial \mathrm{In}v}{\partial \mathrm{In}T}\left(\frac{\partial \mathrm{In}v}{\partial \mathrm{In}T} + \frac{\partial \mathrm{In}v}{\partial \mathrm{In}p} \right) \right]} \tag{24}$$

where v and c_{p} are the specific volume and specific heat at constant pressure of the air–fuel mixture in $\mathrm{cm}^3/\mathrm{gr}$ and kJ/kgK, respectively.

In order to solve the differential equations given above, the modified RATES and STATE codes [31] developed by Gonca [33] are used. These codes give results taking into consideration combustion products assumed at chemical equilibrium with respect to change of crank angle.

In the study, effective values of power and thermal efficiency are used in order to compare the experimental and theoretical results. The effective power and thermal efficiency are expressed as

$$P_{\mathrm{e}} = \frac{W_{\mathrm{e}} N}{120} \tag{25}$$

$$\eta_{\mathrm{e}} = \frac{P_{\mathrm{e}}}{\dot{m}_{\mathrm{f}} H_{\mathrm{u}}} \tag{26}$$

NO emissions are calculated by using extended Zeldovich mechanism taking into account ten combustion products including CO_2, H_2O, N_2, O_2, CO, H_2, H, O, OH and NO

Table 4 Reactions for NO formation [36]

No.	Reactions	Forward/Backward		
		A_A (cm^3/mol s)	B_A	E_A (kcal/mol K)
1	$N_2 + O \leftrightarrow NO + N$	7.6×10^{13} /	0 /	–38000 /
		1.6×10^{13}	0	0
2	$O_2 + N \leftrightarrow NO + O$	6.4×10^{09} /	0 /	–3150 /
		1.5×10^{09}	0	–19500
3	$OH + N \leftrightarrow NO + H$	4.1×10^{13} /	0 /	0 /
		2×10^{14}	0	–23650

[34]. In this study, the ECP code which was developed by Olikara and Borman [35] is modified by adding steam injection and CO_2 into the reactants because CO_2 is dominant gas in the exhaust gas and it can be used for simplification in the computations. The combustion reaction used in the modified program is given below:

$$\begin{aligned}&\varepsilon\phi C_\alpha H_\beta O_\gamma N_\delta + (0.21\,O_2 + 0.79\,N_2) + xH_2O + yCO_2\\&\rightarrow v_1CO_2 + v_2H_2O + v_3N_2 + v_4O_2 + v_5CO\\&+v_6H_2 + v_7H + v_8O + v_9OH + v_{10}NO\end{aligned}$$

where ε is molar fuel–air ratio, which is given as [31]

$$\varepsilon = \frac{0.21}{\alpha + 0.25\beta - 0.5\gamma} \tag{27}$$

The x constant in the reactants is mole fraction of injected steam and can be calculated as

$$X = \frac{Y_{\%} M_{\mathrm{air}}}{M_{\mathrm{ste}}} \tag{28}$$

where M_{air} and M_{ste} are molecular weights of the air and steam. $Y_{\%}$ is ratio of the steam mass to the air mass and defined as

$$Y_{\%} = \frac{m_{\mathrm{ste}}}{m_{\mathrm{air}}} \tag{29}$$

The y constant in the reactants is mole fraction of EGR (CO_2) and can be calculated as

$$y = \frac{Z_{\%} M_{\mathrm{air}}}{M_{\mathrm{co_2}}} \tag{30}$$

where M_{CO2} is molecular weight of CO_2. $Z_{\%}$ is ratio of the CO_2 mass to the air mass and defined as

$$Z_{\%} = \frac{m_{\mathrm{co_2}}}{m_{\mathrm{air}}} \tag{31}$$

The reaction steps for NO formation may be seen in Table 4.

The rate constant is expressed as

$$k = A_{\mathrm{A}} T^{B_{\mathrm{A}}} e^{\frac{E_{\mathrm{A}}}{T}} \tag{32}$$

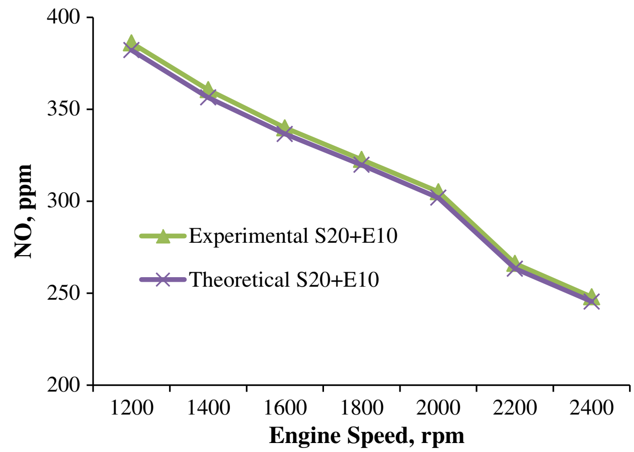

Fig. 2 Comparison of experimental and theoretical results of NO emissions

The rate of NO formation (mol cm^{-3} s^{-1}) is given by [34]

$$\frac{\mathrm{d[NO]}}{\mathrm{d}t} = \frac{2R_1(1-\alpha^2)}{1+\frac{\alpha R_1}{R_2+R_3}} \tag{33}$$

where $\alpha = \frac{[\mathrm{NO}]}{[\mathrm{NO}]_{\mathrm{e}}}$ and $[]_{\mathrm{e}}$ denotes equilibrium concentration. The other constants used in Eq. (33) are

$$R_1 = k_{+1}[\mathrm{N_2}]_{\mathrm{e}}[\mathrm{O_2}]_{\mathrm{e}} = k_{-1}[\mathrm{NO}]_{\mathrm{e}}[\mathrm{N}]_{\mathrm{e}} \tag{34}$$

$$R_2 = k_{+2}[\mathrm{O_2}]_{\mathrm{e}}[\mathrm{N_2}]_{\mathrm{e}} = k_{-2}[\mathrm{NO}]_{\mathrm{e}}[\mathrm{O}]_{\mathrm{e}} \tag{35}$$

$$R_3 = k_{+3}[\mathrm{OH}]_{\mathrm{e}}[\mathrm{N_2}]_{\mathrm{e}} = k_{-3}[\mathrm{NO}]_{\mathrm{e}}[\mathrm{H}]_{\mathrm{e}} \tag{36}$$

4 Results and Discussion

The mathematical model was validated by comparison between the experimental and simulated results for the optimum S20+E10 engine setup [27]. The model validation is illustrated in Figs. 2, 3 and 4 for NO emissions, effective efficiency and effective power, respectively. This study is extended to evaluate the effect of design parameters as CR, IT and pressure on diesel engine performance and emissions. Engine specification is given in Table 5.

A comprehensive parametric study of the effects of design parameters on performance and NO emissions of steam-injected diesel engine with EGR is presented in Figs. 4, 5, 6, 7 and 8. In the study, inlet conditions mean those at the end of suction process and beginning of compression process.

Table 6 illustrates the values of the parametric variables of CR, IT, IP-SER, IP-SFA and Φ. The reference conditions for the engine is 17 for CR, 300 K for IT and 0.9 bar for inlet pressure.

Figure 5 illustrates the effects of variation of engine design parameters on NO emissions at 2,200 rpm. NO emissions

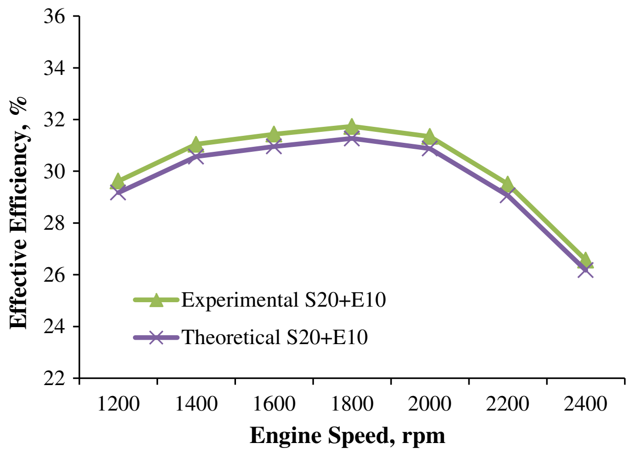

Fig. 3 Comparison of experimental and theoretical results of effective efficiency

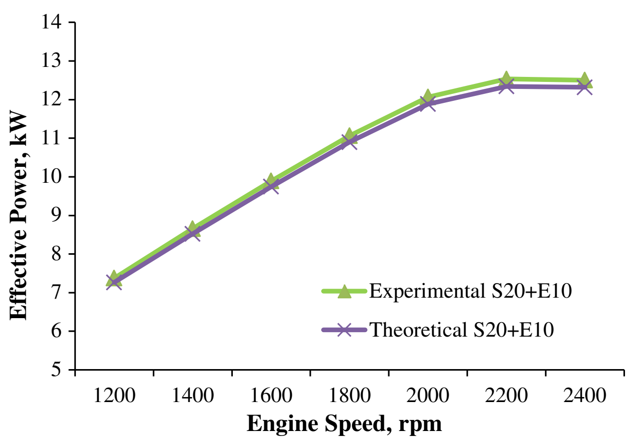

Fig. 4 Comparison of experimental and theoretical results of effective power

Table 5 Engine specifications

Engine type	Super star
Bore (mm)	108
Stroke (mm)	100
Cylinder number	1
Stroke volume (dm^3)	0,92
Power, 1,500 rpm, (kW)	13
Injection pressure (bar)	175
Injection timing, bTDC (crank angle)	35
Compression ratio	17
Maximum speed (rpm)	2,500
Cooling	Water
Injection	Direct injection

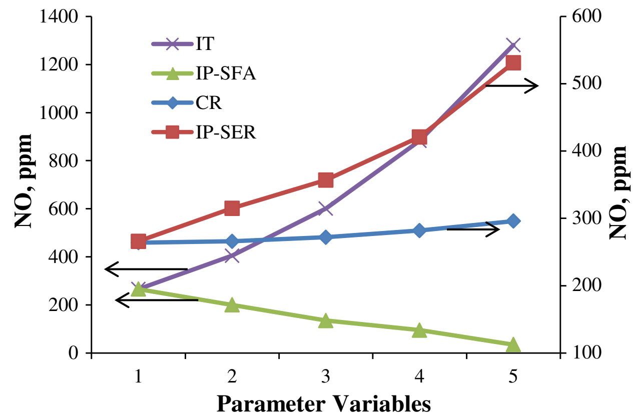

Fig. 5 Parametric comparisons for NO emissions

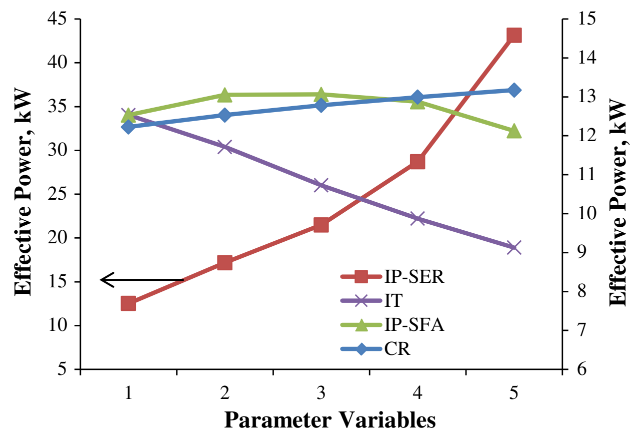

Fig. 6 Parametric comparisons for effective power

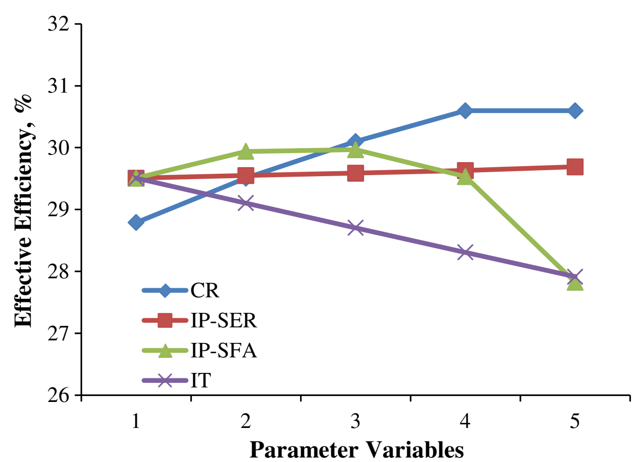

Fig. 7 Parametric comparisons for effective efficiency

increase with the increase of CR, IT and IP-SER. However, with the increase of inlet pressure at same fuel amount (IP-SFA) injected, NO emissions decrease considerably. As can be seen from the Fig. 5, increases of IT and IP-SER more affects in-cylinder temperature and thus NO emissions compared to CR.

Figure 6 shows the effects of variation of engine design parameters on effective power at 2,200 rpm. CR and inlet

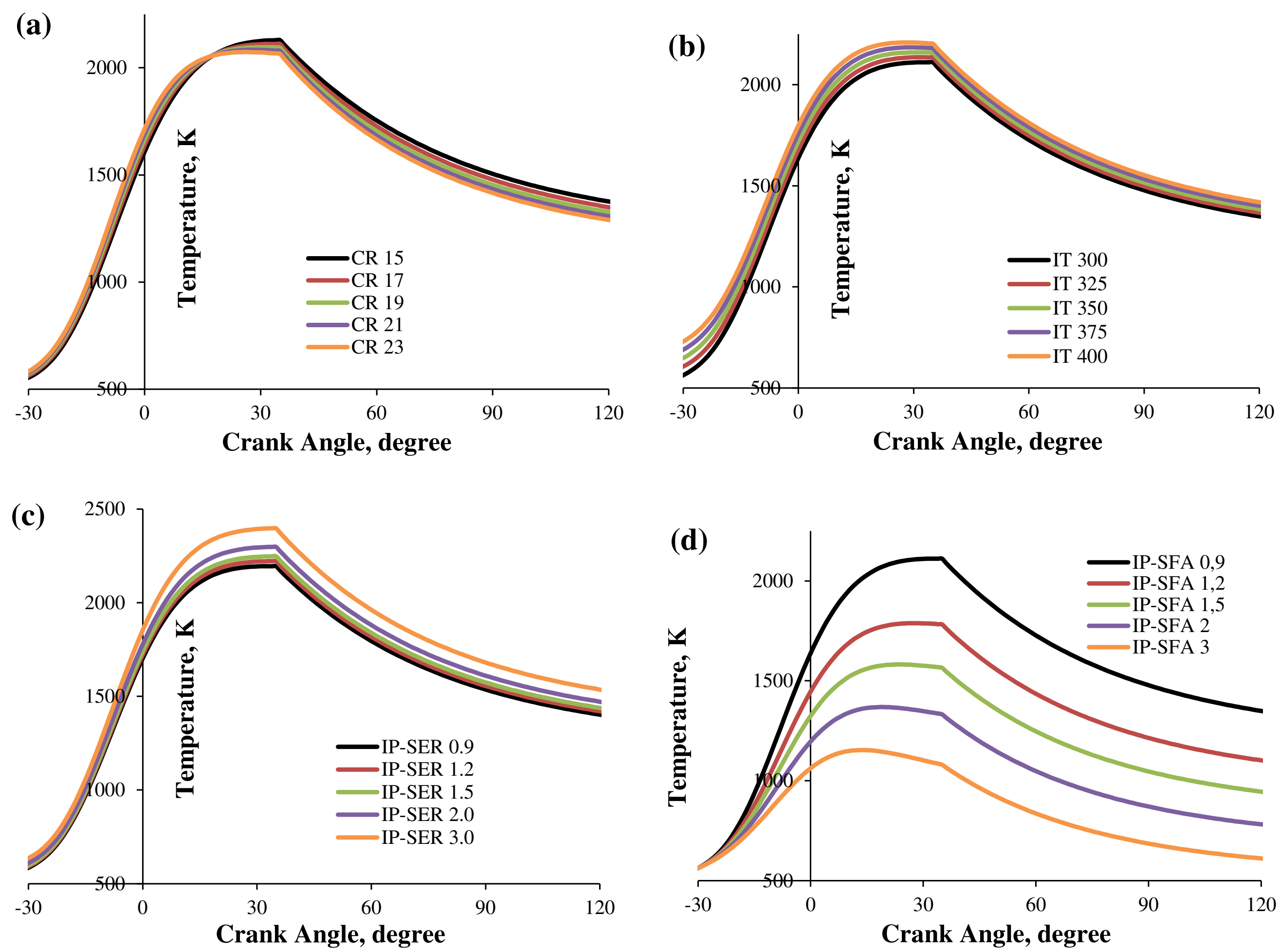

Fig. 8 Variation of gas temperatures with crank angle for various **a** compression ratios (CR), **b** inlet temperatures (IT) **c** inlet pressures at the same equivalence ratio (IP-SER) and **d** inlet pressures at the same fuel amount injected (IP-SFA)

Table 6 Parameter variables

No.	CR	IT (K)	IP-SER (bar) ($\Phi = 0.885$)	IP-SFA (bar)
1	15	300	0.9	0.9 ($\Phi = 0.885$)
2	17	325	1.2	1.2 ($\Phi = 0.7375$)
3	19	350	1.5	1.5 ($\Phi = 0.59$)
4	21	375	2	2 ($\Phi = 0.4425$)
5	23	400	3	3 ($\Phi = 0.295$)

pressure at the same equivalence ratio have a positive effect on the effective power but IT has opposite effect. The effective power rises to certain values and then reduces with respect to variation of inlet pressure at the same fuel amount injected.

Figure 7 indicates the effect of engine design parameters on effective efficiency. It is shown in the figure that there are remarkable changes with the increase of IT and CR. It is obvious that the changing trend is same as that of the effective power.

It is obvious from Figs. 6 and 7 that while effective power and efficiency decrease, NO emissions increase by the increase of IT. The reason for effective power and efficiency reductions is the decrease of volumetric efficiency depending on the IT. The reason of higher NO formation is that higher IT causes to increase in combustion temperature. The figures also show that the effects of inlet pressure on effective power and the efficiency have different characteristics for SER and SFA. Best results are obtained with an increase in inlet pressure for SFA conditions although the mixture becomes leaner compared to SER up to 2.5 bar inlet pressure. This means that the engine consumes lower fuel for the SFA conditions compared to SER. As higher effective power is obtained with a leaner mixture when compared with standard diesel, the effective efficiency also increases up to 2.5 bar inlet pressure. After this pressure, effective power and efficiency of the engine decrease because heating value of the leaner mixture is considerably low.

Figure 8a–d shows the effects of CR, ITs and pressures on temperature variations with crank angle at 2,200 rpm. When

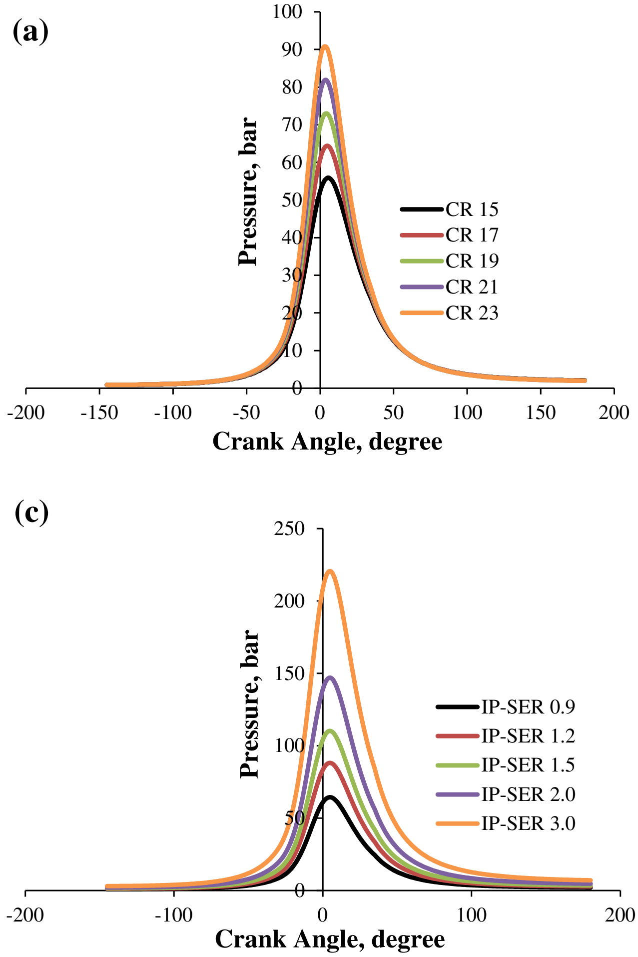

Fig. 9 Variation of gas pressure with crank angle for various **a** compression ratios (CR), **b** inlet temperatures (IT) **c** inlet pressures at the same equivalence ratio (IP-SER) and **d** inlet pressures at the same fuel amount injected (IP-SFA)

CR, IT and IP-SER are considered together, the effects of CR on NO formation rate is limited compared to the other parameters (from Fig. 8a–c). Figure 8d shows the effect of inlet pressure for same fuel amount. The figure illustrates that as the inlet pressure increases peak temperature decreases. This is because the air–fuel mixture becomes leaner while inlet pressure increases.

Figures 9a–d illustrates the effects of CRs, ITs, IP-SER and IP-SFA. The maximum pressure increases with the rise in CR and inlet pressures, but decreases with ITs. The reason of reduction in the peak pressure depending on the IT increase is that less air enters into the cylinder and volumetric efficiency decreases. In-cylinder pressure profiles show different characteristics for inlet pressure at SER and inlet pressure at SFA. Although more fuel enters into the cylinder for inlet pressure at SER condition compared to inlet pressure at SFA condition, in-cylinder pressures are higher. This is why leaner mixture is obtained with the increase of inlet pressure at SFA condition (Fig. 9c, d).

It can be said from Figs. 8 and 9 that as CR increases, pressure increases; rate and peak pressure also increase. This causes an increase in effective power and efficiency. However, increasing CR adversely affects in-cylinder temperature after TDC. As can be known from the literature [34], that NO formation rate depends on three main factors: peak temperature in-cylinder, duration of time that the cylinder gases exposed to higher temperatures and the oxygen content during combustion. As can be seen from Fig. 8a, although peak temperature decreases as the CR increases, NO slightly increases at higher CR values since the duration at the peak combustion temperature is extended after TDC.

5 Conclusion

In this study, an engine with steam injection and EGR has been parametrically investigated on performance and NO emissions using zero-dimensional single-zone combustion model which was previously verified with experimental data.

The parameters used in the study are CR, IT, inlet pressures at same equivalence ratio and for same fuel rate.

NO emissions decrease considerably with the increase of IP-SFA injected, and increase with the increase of CR, IT and pressure at same equivalence ratio. The reason of higher NO formation is that higher IT causes to increase in combustion temperature.

The lowest NO is obtained with increase of inlet pressure for the same fuel amount conditions. The effective power and efficiency continue to increase up to 2.5 bar although the mixture becomes leaner. After 2.5 bar of inlet pressure, effective power and efficiency of the engine decrease because heating value of the leaner mixture is considerably low. The most possible reason for increase in effective power and efficiency by means of steam injection could be explained with the improvement in vaporization and mixing processes which lead to a shorter combustion reaction [13,37]. Furthermore, the improved performance with S20 could be explained owing to the presence of the diesel oil–water steam interface with very low interfacial tension which leads to a finer atomization of the fuel during injection. Higher contact with the air during the burning process resulted in a finer dispersion of the fuel drops. Depression of thermal dissociation could be the third reason for improved combustion efficiency [13,14].

Increase in IT leads to decrease in the effective power as the less air is introduced into the cylinder. The same trend is observed with the increase of CR. As the IT and CR increase, the compression temperature and consequently combustion temperature increase leading to the increase of NO emissions. However, increasing CR and IT shows adverse effects on performance of the engine. Although increasing IT causes a decrease in performance as less air enters into the engine, increasing CR causes to increase performance.

Increasing inlet pressure for the same equivalence ratio adversely affects NO emissions and performance compared to those of inlet pressure for the same amount of fuel injected. This is because increasing inlet air pressure also means to increase fuel amount injected into the cylinder. As more fuel enters into the cylinder, higher effective power and NO emissions occur.

Acknowledgments This study was supported by TUBITAK 1001 Project (Project No. 111M065) and Yildiz Technical University (YTU) Scientific Research Project Coor.(SRPC) (BAPK) (Project No. 2011-10-02-KAP02). Thanks to TUBITAK and YTU SRPC for the financial support.

References

1. Rakopoulos, C.D.; Dimaratos, A.M.; Giakoumis, E.G.; Rakopoulos, D.C.: Evaluation of the effect of engine, load and turbocharger parameterson transient emissions of diesel engine. Energ. Convers. Manage. **50**, 2381–2393 (2009)
2. Jayashankara, B.; Ganesan, V.: Effect of fuel injection timing and intake pressure on the performance of a DI diesel engine—a parametric study using CFD. Energ. Convers. Manage. **51**, 1835–1848 (2010)
3. Kim, H.J.; Park, S.H.; Lee, K.S.; Lee, C.S.: A study of spray strategies on improvement of engine performance and emissions reduction characteristics in a DME fueled diesel engine. Energy **36**, 1802–1813 (2011)
4. Samec, N.; Breda, K.; Dibble, R.W.: Numerical and experimental study of water/oil emulsified fuel combustion in a diesel engine, effects of direct water injection on DI diesel engine combustion. Fuel **81**, 2035–2044 (2002)
5. Bedford, F.; Rutland, C.; Dittrich, P.; Raab, A.; Wirbelit, F.: Effects of direct water injection on DI diesel engine combustion. SAE Paper 2000-01-2938
6. Park, J.W.; Huh, K.Y.; Lee, J.H.: Reduction of NOx, smoke and brake specific fuel consumption with optimal injection timing and emulsion ratio of water-emulsified diesel. P. I. Mech. Eng. D-J. Aut. **215**, 83–93 (2001)
7. Armas, O.; Ballesteros, R.; Martos, F.J.; Agudelo, J.R.: Characterization of light duty diesel engine pollutant emissions using water-emulsified fuel. Fuel **84**, 1011–1018 (2005)
8. Dryer, F.L.: Water addition to practical combustion systems—concepts and applications. Symposium (international) on combustion **16**, 279–295 (1977)
9. Lin, C.Y.; Wang, K.H.: Diesel engine performance and emission characteristics using three-phase emulsions as fuel. Fuel **83**, 537–545 (2004)
10. Tauzia, X.; Maiboom, A.; Shah, S.R.: Experimental study of inlet manifold water injection on combustion and emissions of an automotive direct injection diesel engine. Energy **35**, 3628–3639 (2010)
11. Abu-Zaid, M.: Performance of single cylinder, direct injection diesel engine using water fuel emulsion. Energ. Convers. Manage. **45**, 697–705 (2004)
12. Alahmer, A.; Yamin, J.; Sakhrieh, A.; Hamdan, M.A.: Engine performance using emulsified diesel fuel. Energ. Convers. Manage. **51**, 1708–1713 (2010)
13. Parlak, A.; Ayhan, V.; Üst, Y.; Şahin, B.; Cesur, Ý.; Boru, B.; Kökkülünk, G.: New method to reduce NOx emissions of diesel engines: electronically controlled steam injection system. J. Energy Inst. **85**, 135–139 (2012)
14. Parlak, A.; Ayhan, V.; Üst, Y.; Şahin, B.; Cesur, Ý.; Boru, B.; Kökkülünk, G.: The effects of the new developed electronic controlled steam injection system on NOx emissions of a single cylinder diesel engine. 13th international conference maritime transport and infrastructure, Riga, p. 139–144 (2011)
15. Murthy, Y.V.V.S.; Sastry, G.Y.K.; Satyanaryana, M.R.S.: Experimental investigation of performance and emissions on low speed diesel engine with dual injection of solar generated steam and pongamia methyl ester. Indian J. Sci. Technol. **4**, 29–33 (2011)
16. Heffel, J.W.: NOx emission reduction in a hydrogen fuelled internal combustion engine at 3000 rpm using exhaust gas recirculation. Int. J. Hydrogen Energ. **28** 1285–1292 (2003)
17. Selim, M.Y.E.: Effect of exhaust gas recirculation on some combustion characteristics of dual fuel engine. Energ. Conver. Manage. **44**, 707–721 (2003)
18. Zheng, M.; Reader, G.T.; Hawley, J.G.: Diesel engine exhaust gas recirculation—a review on advanced and novel concept. Energ. Convers. Manage. **45**, 883–900 (2004)
19. Pirouzpanah, V.; Saray, K.R.; Sohrabi, A.; Niaei, A.: Comparison of thermal and radical effects of egr gases on combustion process in dual fuel engines at part loads. Energ. Convers. Manage. **48**, 1909–1918 (2007)
20. Saleh, H.E.: Experimental study on diesel engine nitrogen oxide reduction running with jojoba methyl ester by exhaust gas recirculation. Fuel **88**, 1357–1364 (2009)

21. Maiboom, A.; Tauzia, X.; Hetet, J.F.: Experimental study of various effects of exhaust gas recirculation (EGR) on combustion and emissions of an automotive direct injection diesel engine. Energy **33**, 22–34 (2008)
22. Kiplimo, R.; Tomita, E.; Kawahara, N.; Yokobe, S.: Effects of spray impingement, injection parameters, and egr on the combustion and emission characteristics of a PCCI diesel engine. Appl. Therm. Eng. **37**, 165–175 (2012)
23. Nathan, S.S.; Mallikarjuna, J.M.; Ramesh, A.: Effects of charge temperature and exhaust gas re-circulation on combustion and emission characteristics of an acetylene fuelled HCCI engine. Fuel **89**, 515–521 (2010)
24. Peng, H.; Cui, Y.; Shi, L.; Deng, K.: Effects of Exhaust gas recirculation (EGR) on combustion and emissions during cold start of direct injection (DI) diesel engine. Energy **33**, 471–479 (2008)
25. Shi, L.; Cui, Y.; Deng, K.; Peng, H.; Chen, Y.: Study of low emission homogeneous charge compression ignition (HCCI) engine using combined internal and external exhaust gas recirculation (EGR). Energy **31**, 2665–2676 (2006)
26. Ladommatos, N.; Abdelhalim, S.M.; Zhao, H.; Hu, Z.: The effects of carbon dioxide in exhaust gas recirculation on diesel engine emission. P. I. Mech. Eng. D-J. Aut. **212**, 25–42 (1998)
27. Kökkülünk, G.; Parlak, A.; Ayhan, V.; Cesur, Ý.: Investigation of steam injection with exhaust gas recirculation (EGR) on a diesel engine, 3rd international conference on urban sustainability, cultural sustainability, green development, green structures and clean cars (USCUDAR \'12), Barcelona, pp. 41–46 (2012)
28. Needham, J.R.; Nicol A.J.; Such C.H.: Low emission heavy duty diesel engine for Europe. SAE Paper, 620–631 (1993)
29. Çetinkaya S.: Termodinamik. Ankara: Nobel Yayınları; (1999) (in Turkish)
30. Kökkülünk, G.; Gonca, G.; Ayhan, V.; Cesur, I.; Parlak A.: Theoretical and experimental investigation of diesel engine with steam injection system on performance and emission parameters. Appl. Therm. Eng. **54**, 161–170 (2013)
31. Ferguson, R.: Internal combustion engines—applied thermodynamic, pp. 180–187. Wiley, New York (1986)
32. Hohenberg, G.: Advanced approaches for heat transfer calculations, SAE Paper 790825 (1979)
33. Gonca, G.: Investigation of the effects of steam injection into the supercharged diesel engine with running miller cycle on performance and emissions. PhD Thesis Progress Report (2011)
34. Heywood, J.B.: Internal combustion engine fundamentals. McGraw-Hill Inc., New York (1988)
35. Olikara, C.; Borman, G.: A computer program for calculating properties of equilibrium combustion products with some applications to the engines. SAE Paper 750468 (1975).
36. Gonca, G.; Sahin B.; Ust Y.; Parlak A.: A study on late intake valve closing miller cycled diesel engine. Arab. J. Sci. Eng. **38**(2), 383–393 (2013)
37. Mello, J.P.; Mellor, A.M.: NOx emissions from direct injection diesel engines with water/steam dilution, SAE J-Automot. Eng. 01–0836 (1999)